PERFORMANCE OF A LEAD–GLASS ELECTROMAGNETIC SHOWER DETECTOR AT FERMILAB

J. A. APPEL, M. H. BOURQUIN*, I. GAINES†. D. C. HOM, L. M. LEDERMAN, H. P. PAAR, J.-P. REPELLIN+, D. H. SAXON§, H. D. SNYDER, J. M. WEISS, J. K. YOH

*Columbia University, Irvington on Hudson, New York 10533**, USA*

and

B. C. BROWN, C. N. BROWN, J.-M. GAILLARD+, J. R. SAUER and T. YAMANOUCHI

Fermi National Accelerator Laboratory, Batavia, Illinois 60510††, USA

Received 26 May 1975

The performance of a lead–glass spectrometer system with high resolution and superior hadron rejection is described. We present results on calibration, energy resolution and stability. The use of the system in triggering and in the analysis of an experiment measuring electrons in the energy range 15 to 100 GeV at Fermilab are also described.

1. Introduction

Calorimeters have played an increasingly important role in high energy physics experiments. This is due primarily to the increased resolution possible with higher energy incident particles. Over the past year and a half, we have been measuring high energy electrons (15–100 GeV) at the Fermi National Accelerator Laboratory using a lead–glass total absorption electromagnetic shower detector. These measurements extend the lead glass calorimeter technique to a new energy and resolution domain.

Lead–glass is a nearly ideal electromagnetic shower detector, a transparent material with high average Z. The high Z of the lead–glass insures the rapid development of a cascade shower upon the entrance of an electron, positron or photon into the detector. The clarity of the glass allows nearly complete sampling of the energy deposited in the detector. The relativistic charged particles in the electromagnetic cascade emit Cherenkov radiation which is transmitted through the glass and is collected in photomultiplier tubes. The total path length of the particles in the shower is proportional to the energy of the incident particle and, thus, the total Cherenkov light is proportional to the energy of the showering particle.

Lead glass is sufficiently dense that manageable amounts will contain the electromagnetic showers of electrons and photons at available energies. It is nevertheless both convenient and useful to modularize the detector. In such arrays it is crucial that the amount of light collected in each module corresponds uniquely to the total energy deposited in that module, independent of the details of the manner in which the energy was deposited.

Tests of this technique at lower energies have been reported previously[1]). We report here on the performance of a lead–glass detector at Fermilab. Energy resolution of $(1.5+10/\sqrt{E})\%$ fwhm (E in GeV) is obtained over the entire aperture of our large array with a uniformity of better than $\pm\frac{1}{2}\%$. Corrections are applied to raw data to maintain this result independent of time or entry point in the detector. Used in conjunction with a magnetic spectrometer, the lead–glass gives a hadron rejection in off-line analysis of better than 10^5. In addition, it provides fast triggering information sufficient to reject hadrons on-line to better than 1 in 10^3.

2. Description of the calorimeter

The lead–glass is type SF5* with properties as listed in tables 1 and 2. Our detector uses 45 identical blocks, each $15\times15\times35\ \mathrm{cm}^3$. Smaller blocks would give better spatial resolution, but would be substantially

* Present address: Université de Genève, Genève, Switzerland.
† Present address: Fermi National Accelerator Laboratory, Batavia, Illinois 60510, USA.
\+ Permanent address: Laboratoire de l'Accélérateur Linéaire, Orsay, France.
§ Present address: Rutherford High Energy Laboratory, Chilton, Berkshire, England.

** Work supported in part by the National Science Foundation and the Energy Research and Development Administration.
†† Work supported by the Energy Research and Development Administration.

* Type 673321 manufactured by Ohara Optical Glass Co., Tokyo, Japan.

TABLE 1

Properties of lead–glass.

Type	SF5
Composition (by weight)	55% PbO
	38% SiO_2
	5% K_2O
	1% Na_2O
Radiation length	2.36 cm
Critical energy	15.8 MeV
Refractive index	1.67270
Specific gravity	4.08
Thermal expansion coefficient	85×10^{-7}
	(−30° to +70 °C)

TABLE 2

Internal transmission of 25 mm thickness of lead–glass.

λ (Å)	Transmission (%)
3400	2
3500	27
3600	57
3700	75
3800	85
3900	92
4000	95
4200	97.5
4400	98
5000	99
7000	99.3

more expensive for the same detector volume and would also have more "cracks" between blocks.

An RCA 8055 photomultiplier tube (PM) is glued to each block with KODAK HE-10 assembly cement (index of refraction 1.58). The tubes were selected from a sample of 500 for uniformity of gain and good quantum efficiency**. The tubes are run at negative high voltage so that the anode signals can be DC coupled. The blocks are wrapped first with soft aluminum foil (thickness 0.001″) which extends the cathode high voltage around the glass block to prevent leakage currents across the photocathode, then with mylar (0.005″) for electrical insulation and finally with black polyethylene (0.006″) for optical isolation.

The gain of the 10-stage PM is kept low in order to assure linearity of the PM response over a large dynamic range. Rather than lower the overall operating voltage with a linear chain, extra voltage is provided by the first few and last few stages of the voltage divider as shown in fig. 1. The extra voltage in the first few stages is to provide uniformity of response over the photo-

** We would like to thank Prof. C. Rubbia for allowing us to select the best phototubes from his stock.

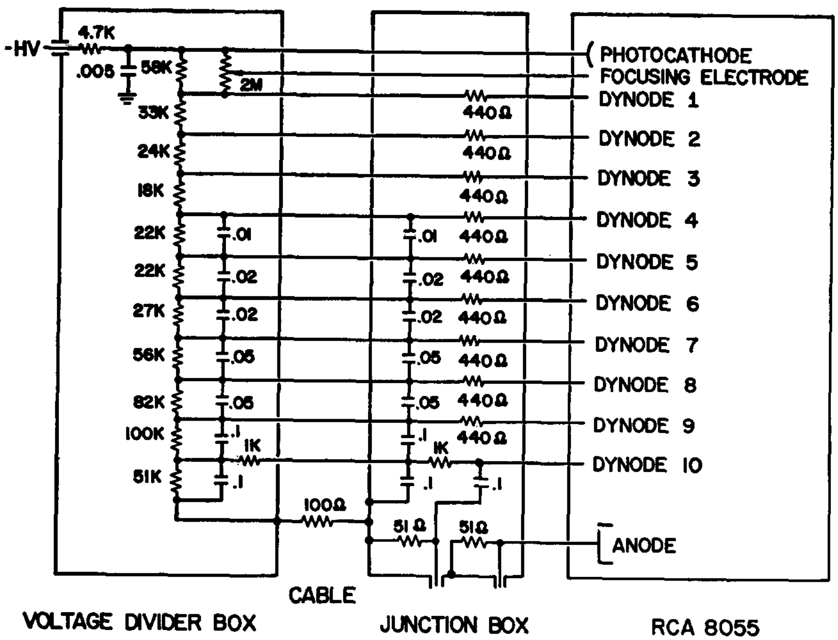

Fig. 1. Circuit diagram of photomultiplier base designed for uniform collection efficiency, low gain and linear response with −1500 V applied.

cathode and in the last few stages to improve linearity at the highest output currents. Peak output currents are 0.16 mA per GeV with fwhm of 80 ns. The integral non-linearity was measured to be 1% for 40 mA peak current.

The light output from each block of lead–glass is recorded separately. The anode current from each phototube is integrated over a 270 ns gate for each event and digitized in an analog-to-digital converter*. The digitizers are equipped with a base line correction circuit which clamps the input stage to the most positive level and with a pedestal injection circuit which puts the input data into the most linear part of the digitizer response. Typical settings of the variable gain were 500 pC for 1024 channels full scale during data taking and 25 pC full scale for special muon calibration runs. This latter high gain requires special care to minimize ground loop currents in the 70 m cables from the lead–glass array to the digitizers. The digitizer circuitry is isolated from local grounds, the high voltage ground has a 100 Ω standoff resistor from the common of the photomultiplier base and the dynode outputs have isolation transformers in them. The dynode signals from the blocks are summed and amplified to provide an electron trigger. This allows a selection at the trigger formation time of those events which deposit large amounts of energy in the lead–glass.

The blocks are arranged as shown in fig. 2. to provide three layers of 6.2, 6.2, and 14.8 radiation lengths along the beam direction. The detector covers a cross-sectional area of 75 cm × 75 cm, but since particles entering near an edge of the array must be excluded due to possible energy leakage out of the array, we use a fiducial area of 60 cm × 60 cm external dimensions. In addition, a 5 cm wide vertical strip at the center of the array is excluded due to a 1 cm gap between the right and left halves of the first two rows of glass for insertion of a light distribution sheet for a light flasher calibration system. A curtain of scintillation counters (T2) between the first and second layers of glass provides triggering information.

In front of the array is a sheet of lead 2.3 radiation lengths (1.3 cm) thick, with scintillation counters in front (D) and behind (E). The pulse areas from the individual T2, D, and E counter signals are digitized and recorded for each event.

The entire detector has 29 radiation lengths, more than sufficient to contain the complete electromagnetic shower, yet only 1.6 absorption lengths. Hodoscopes which are located immediately in front of the array specify the entry point into the array to ±3 mm. The array is enclosed in a thermally insulated box with walls made of aluminum-clad 2.5 cm styrofoam. All significant heat sources are outside the box. In particular, the resistor chain with its standing current for each photomultiplier is mounted outside the box and connected to the photomultiplier socket with extender cables. The response time of the inside of the box to outside temperature changes is greater than 4 h. The temperature in the room surrounding the box is maintained with conventional thermostatically controlled heaters and air conditioners without creating fluctuations in the environment inside the box. The temperature inside the box is continuously monitored by recording the voltage drop across a series of thermistors and across a length of high temperature coefficient wire driven by a constant current source.

3. Calibration and stability of lead glass array

After initial exposure of the lead glass array in its final configuration to an electron beam at Brookhaven National Laboratory and a test run at Fermilab near the final experimental setup, a relationship was determined between muon straight-through signals and the signals for electron showers in units of energy deposited. During the experiment, data are taken with electron-enriched beams (obtained by inserting thin foils in the secondary beam upstream of the spectrometer magnet) and with muons. The muon data serve to monitor the relative gains of the three layers of glass (block by block) and the overall gain is fixed by the requirement that the total signal from a momentum-analyzed electron be equal to its incident energy.

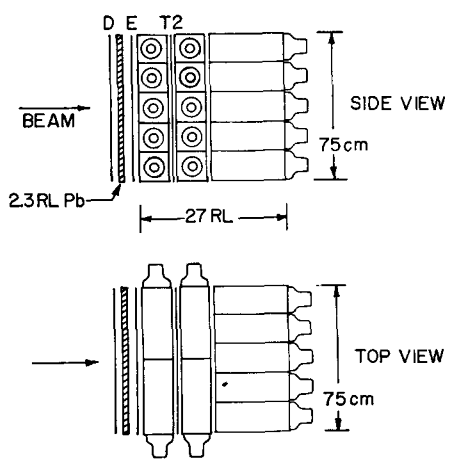

Fig. 2. Diagram of the lead–glass electromagnetic shower detector.

* Designed and constructed at the Nevis Laboratories of Columbia University (F. W. Sippach, to be published).

The relationship between photomultiplier signal and energy deposited in the glass (calibration constant) was obtained for each block by studying a large sample of electron showers in the lead–glass array. We seek calibration constants for which each block has a signal which is proportional to the energy deposited,

$$E_{ij} = \alpha_j A_{ij}, \tag{1}$$

where α_j is the calibration constant for the jth block, E_{ij} is the energy deposited in the jth block and A_{ij} is the signal from the jth block for the ith electron. The sum of all deposited energy must equal the incident energy

$$E_i = \sum_j E_{ij} = \sum_j \alpha_j A_{ij}. \tag{2}$$

Multiplying eq. 2 by A_{ik} and summing over events yields eq. 3:

$$\sum_j \alpha_j X_{jk} = \sum_i E_i A_{ik}, \tag{3}$$

where

$$X_{jk} = \sum_i A_{ij} A_{ik}. \tag{4}$$

Solving eq. 3 for the α_j yields a set of equations (eq. 5) whose solution provides enough information to obtain the relative calibration constants with an overall normalization fixed by eq. 2:

$$\alpha_l = \sum_k \left(\sum_i E_i A_{ik}\right)(x_{kl}^{-1}), \tag{5}$$

with

$$\sum_k X_{jk} X_{kl} = \delta_{jl}. \tag{6}$$

This solution is mathematically identical to that obtained by minimizing the energy resolution subject to the constraint that the total energy equal the incident energy.

In order for this set of linear equations to be independent so that a solution can be found, the shower must be distributed differently among the blocks in different events. The fluctuations evident in fig. 10 are large relative to the resolution in each block. These fluctuations easily satisfy the condition for solution.

Our method of gain monitoring utilizes straight-through muons, which generate a fixed amount of light in each block of glass due to their Cherenkov radiation. The amount of light is proportional to the path length of the muon in the block of glass. Exposing the array to muons near the same time as the electron calibration described above established an equivalent electron energy for the signal given by muons traversing the lead glass blocks. The equivalent muon straight-through energy is observed to be the same for all blocks having the same orientation with respect to the incident particles. The front layers give 132 MeV for 146 mm path length and the back layer gives 550 MeV for 350 mm of path length. The lack of proportionality to path length when the orientation is changed is attributed to the difference in light collection efficiency for the directional Cherenkov radiation. Using this muon equivalent energy allows one to calibrate the entire array with muons very quickly during the running. The gain of each block is monitored in this way by taking muon data approximately once every two days during data acquisition.

Intermediate time stability of the gains is monitored with a light flasher system. A single hydrogen thyratron tube* is viewed by each of the 45 blocks of glass through an opening in the wrapping of each block at the end far from the photomultiplier tube. The light is transmitted to the blocks by a combination of acrylic rod and sheets. The flasher is also viewed by four normalization tubes without glass, but which are fitted with small crystals of NaI(Tl) with ^{241}Am alpha emitters**. These serve to give an absolute normalization to the light flasher calibration. Each block has its signal divided by the value recorded from the normalization tubes. This technique reduces the tens of a percent rms width of the light output to a one to two percent rms variation in the ratio of light seen by various blocks. The absolute gain of the calibration tube is monitored by the signals from the NaI outputs. This light flasher system is stable over short periods but is found inferior to the muon straight-through method over long periods of time. A short term check was made of the validity of the light flasher monitoring scheme. A sample of photomultiplier tube voltages were lowered by 50 V and the light flasher and muon straight-through calibrations were performed. The gain changes (approximately 16%) monitored by muons and light flasher during these tests agreed to better than $\pm 1\%$ and showed no systematic differences.

With voltage and temperature held constant the absolute gain of the blocks was observed to decrease by about 1% per month of beam time. The total radiation absorbed by the blocks was on the order of 35 R (as measured by thermoluminescent diodes†) over

* Krytron Tube (KN22) manufactured by EG&G, Electronic Products Division, Boston, Massachusetts, 02215.

** Integral Light Pulsers, Harshaw Chemical Co., Crystal and Electronic Products Dept., Solon, Ohio 44139.

† Lithium fluoride thermoluminescent dosimeters, Harshaw Chemical Co., Crystal and Electronic Products Dept., Solon, Ohio.

the course of the entire experiment. The average total change in gain response over this same period was 10%.

4. Energy calculation

In principle the energy deposited in the lead glass array is calculated by simply adding the signals from each of the 45 blocks corrected for relative gain. However, dramatic improvements in energy resolution can be achieved by a slightly more sophisticated calculation.

As many blocks as possible are excluded from the energy sum to avoid degrading the resolution with energy from particles not associated with the triggering particle shower. The sum is thus restricted to those blocks within a specific distance of the entry point as determined by the hodoscope in front of the lead glass. In order to compensate for the spreading of the shower as it developed the distances are increased from the first to the last layer of glass. Blocks within 5, 5.6 and 6.3 cm of the entering trajectory are used in the sum for the first, second and third layers, respectively.

Significant improvement in resolution is obtained by applying three corrections to the signals used in the sum. A transit correction is applied to the signals from blocks in the first two layers to account for the different attenuation of light for particles entering at different horizontal positions (and therefore different distances from the photomultiplier). The correction is shown in fig. 3.

A second correction is applied to compensate for energy leakage in the 0.6 cm gaps between adjacent blocks of the last two layers. The correction is typically 2% within 1 cm from the edge of the glass.

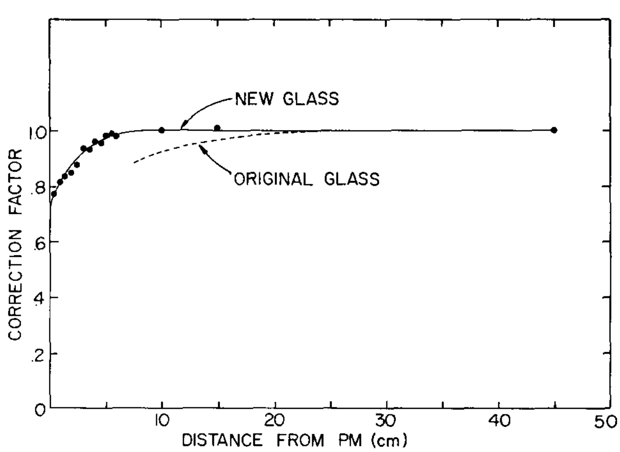

Fig. 3. Transit correction factor vs. point of entry relative to far end of glass. The dashed curve is for the original glass (average of the 20 clearest blocks which were used in the first two layers) The solid curve is for the newer glass as obtained with muons.

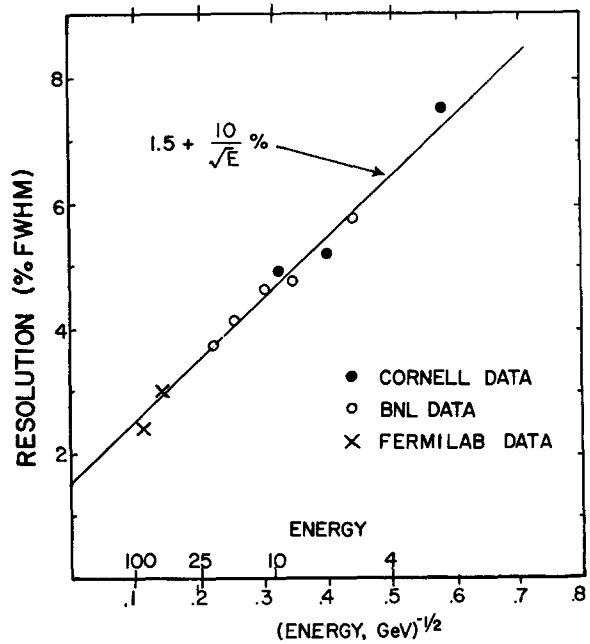

Fig. 4a. SF5 lead glass resolution vs. energy, measured with a limited number of blocks in monochromatic test beams.

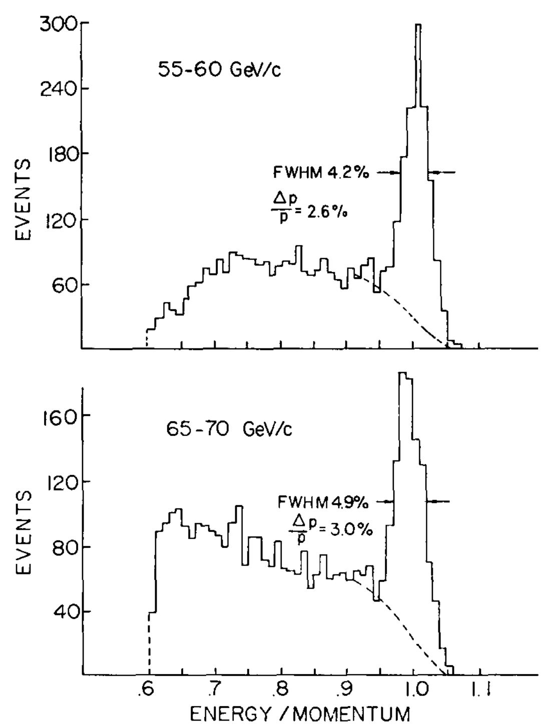

Fig. 4b. Energy resolution for the array as a whole is checked by examining the energy divided by momentum distribution for electrons as indicated.

Finally, different entry points have different numbers of blocks included in the sum, and thus different amounts of leakage outside the included blocks. An additional correction is made for this effect, adding 1.4% when only one rather than two horizontal rows are included in the sum and adding 0.4% when only one vertical column of third row blocks are included in the sum. The correction is additive because the calibration constants are based on adding two rows and two columns, or a total of 8 out of the 45 blocks.

The result of all these corrections is a uniformity in energy as a function of entry position which is better than $\pm 0.5\%$. The energy resolution is then limited only by the statistics of shower development and light collection. The energy resolution was measured in monochromatic charged test beams and checked during data taking (where the momentum resolution prevents precise measurement). Fig. 4a shows the resolution obtained with a limited number of blocks in the various test beams. The resolution can be described by the expression $(1.5 + 10/\sqrt{E})\%$ fwhm for energy E in GeV. Fig. 4b shows the energy resolution of the entire array for two momentum bins. The widths of these curves are due to the combination of the momentum resolution of the magnetic spectrometer and the energy resolution of the lead glass array.

Energy resolution is degraded by fluctuations in any energy which escapes from the calorimeter. For this reason, the full array depth is used to sum the energy. Fig. 5 shows the energy resolution obtained using 12.4

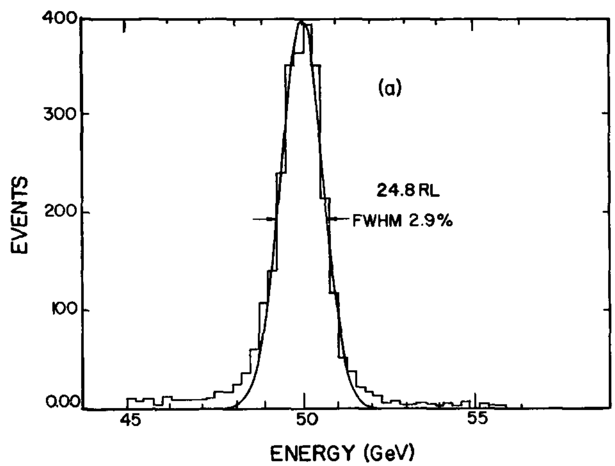

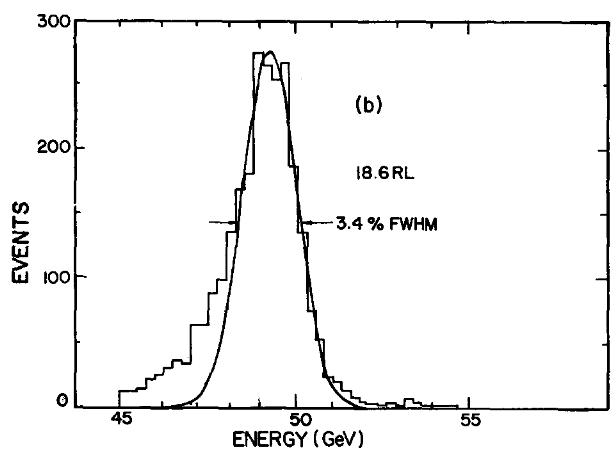

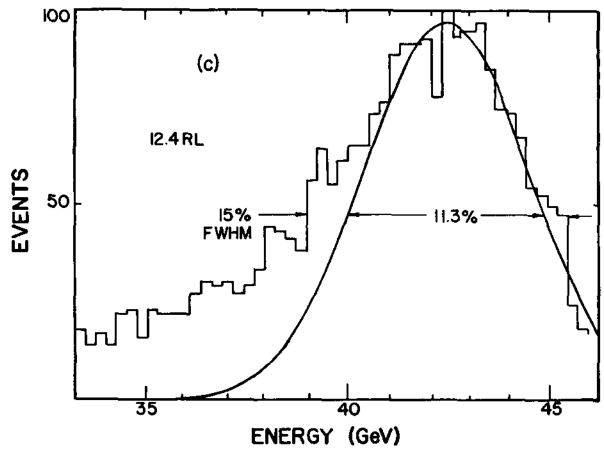

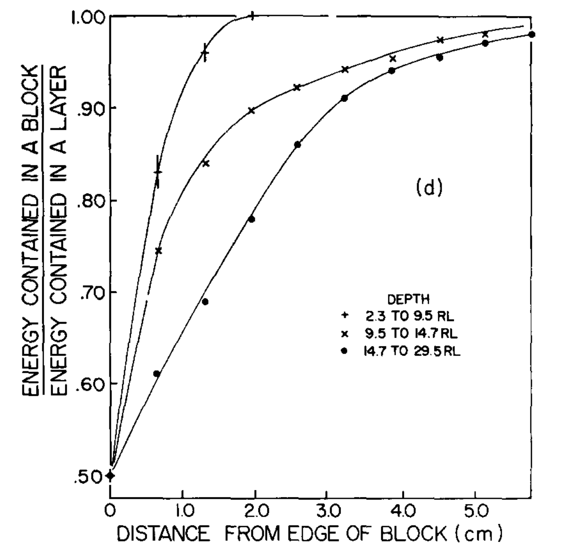

Fig. 5. Energy deposited by 50 GeV electrons in (a) four layers of 6.2 radiation lengths of lead glass without 2 radiation lengths in front, (b) in the first three layers and (c) in the first two layers of glass. (d) Fraction of energy in a layer contained in one block vs. entry point. The smooth curves are gaussian fits with fwhm as indicated.

18.6, and 24.8 radiation lengths of glass*. The resolution obtained with 24.8 radiation lengths was equivalent to the resolution of the 27 radiation length array (with and without the additional 2.3 radiation lengths of lead).

The lateral spread of the electromagnetic shower can be observed by measuring the fraction of energy from one layer which is deposited in one block of that layer. This fraction is plotted in fig. 5d for blocks in each of the three layers as a function of the distance from the edge of the block to the trajectory of entering 40–45 GeV electrons.

5. Use in triggering

The T2 counters are located near the peak of the high energy electromagnetic showers. These scintillation counters are equipped with RCA 6655A 2-inch photomultiplier tubes which have much faster transit and rise times than the 5-inch 8055 photomultiplier tubes of the lead–glass. The signals from the T2 counters are, therefore, convenient to use in generating a loose, early trigger to the slower electronics which follow. Fig. 6 shows the pulse area distribution in these counters for 40 to 45 GeV incident particles which pass the loose requirement. The electrons which enter have significantly more signal. The threshold is kept low in order to be efficient for electrons at all energy ranges detected and to be independent of typical gain variations of the tubes.

* We would like to thank the members of the California Institute of Technology – Fermilab neutrino experiment, for their assistance in obtaining these data.

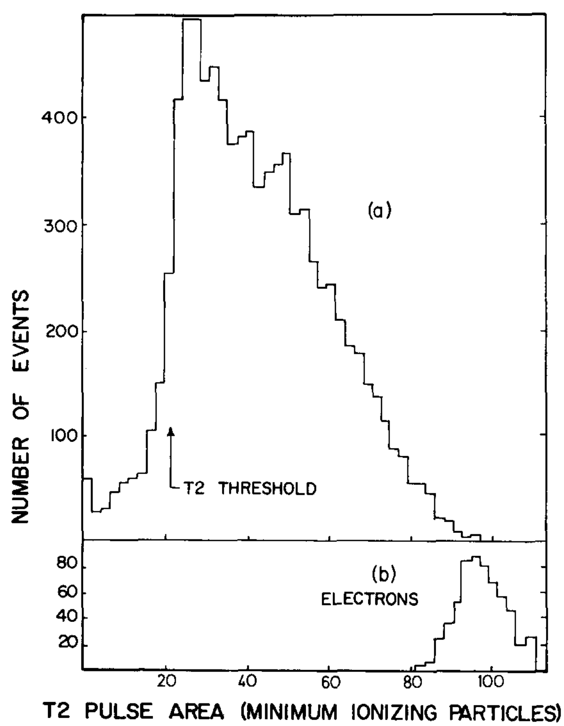

Fig. 6. T2 counter pulse height distribution for 40–45 GeV particles (a) passing the loose trigger requirement and (b) identified as electrons.

The dynode signals from the twenty blocks in the first two layers of lead glass are passively added, amplified and then discriminated at three separate levels: low, medium and high. These are used to create three distinct electron triggers.

The low and middle triggers are prescaled so that rates are more nearly equal over the entire range of momentum available, despite the several orders of magnitude difference in cross sections at the two ends of the spectrum. The efficiencies of these three levels are shown in fig. 7 for a typical running condition along with the geometrical acceptance. The low threshold is 100% efficient over the entire acceptance and serves primarily as a continual check on the efficiency of the two higher thresholds.

6. Hadron rejection

In addition to its use in measurement of the energy of an electromagnetic shower and provision of a trigger which indicates the occurrence of the shower, the lead–glass array serves a vital function in identifying electrons amid a large flux of hadrons. The size of this task in our experiment is indicated by fig. 8a, which plots the energy deposited in the glass divided by the momentum, E/p (i.e., the fraction of a particle's energy it leaves in the lead–glass), for incident charged

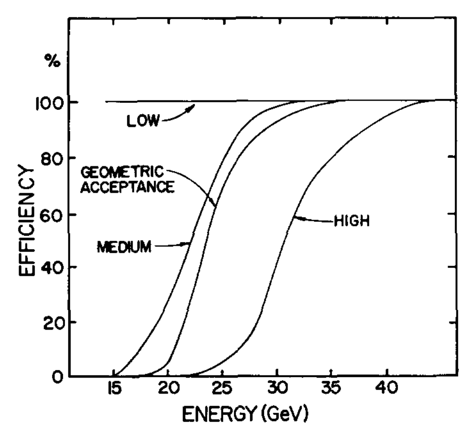

Fig. 7. Trigger efficiencies of the energy thresholds in the sum of the front two layers vs. energy for a typical setting. The geometrical acceptance for this running condition is also shown.

particles. Electrons, which leave all of their energy in the glass, are expected to appear as a peak near 1.0 on this plot, but any small peak is obscured by the tail of the much more abundant hadrons, which usually leave only a fraction of their energy in the glass and thus appear to the left of 1.0 on the *E*/*p* plot.

Part of the hadron rejection is accomplished by the thresholds in the electron trigger as described above. The result of applying these threshold cuts (hadron rejection by a factor of ~500) is shown in fig. 8b where there is a suggestion of an electron peak near 1.0 on the *E*/*p* plot. In order to further separate electrons from those hadrons which deposit all their energy in the array, we use information on the longitudinal distribution of the electromagnetic shower. Two highly correlated kinds of information are used to identify these background hadrons.

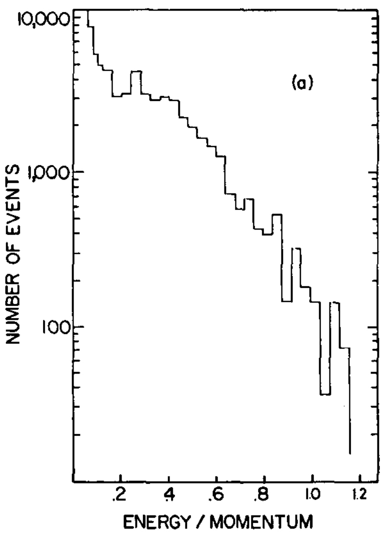

The first of these is the pulse area in the E counters, which are located just in front of the lead glass and behind 2.3 radiation lengths of lead. Demanding off-line a large pulse integral in the E counters insures that the shower starts in these first radiation lengths. Fig. 9 shows the effect on pions and on electrons of a cut on the E counter pulse at various levels. Putting the cut at 7 minimum ionizing particles yields a hadron rejection of 70% while cutting less than 5% of the electrons. We first put a cut on the D counter pulse height to insure that only a single minimum ionizing particle enters the lead.

The second kind of information is the energy distribution in the three rows of lead–glass. Fig. 10 shows the percentage of energy deposited in the first, second, and third rows of glass for electrons and for the background hadrons. Off-line cuts on these quantities give additional hadron rejection. These cuts are a function of energy, since the rate of shower development depends on energy. Fig. 11 shows the variations in the median energy deposit in the three rows of glass as a function of energy. The widths of the curves in fig. 10 are a measure of the fluctuations in the shower development.

The result of these cuts is the *E*/*p* distribution shown in fig. 8c, where a clear electron peak is visible. The

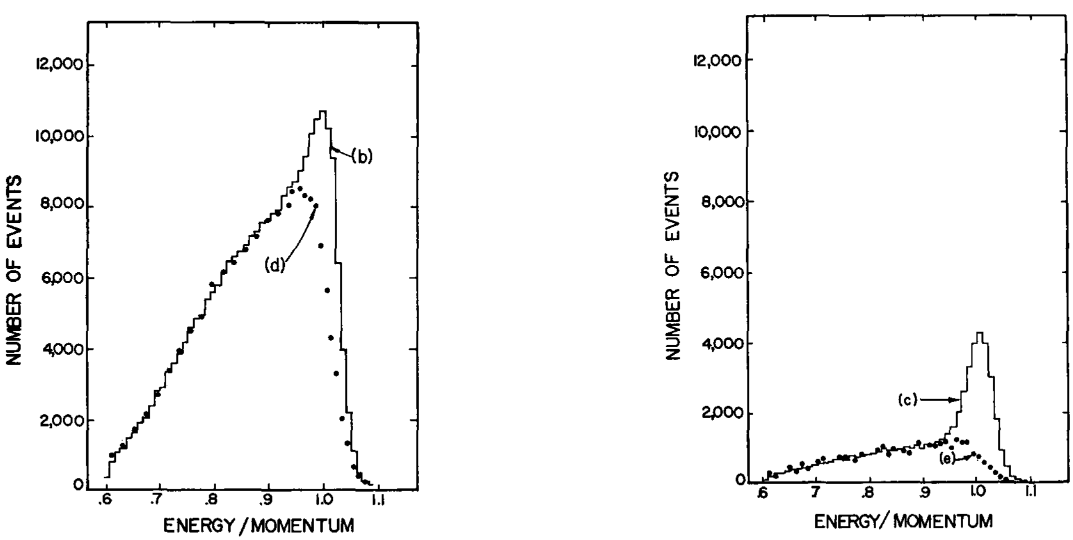

Fig. 8. Fraction of energy deposited in lead glass for (a) all incident charged 40–45 GeV particles, (b) all particles passing the medium threshold trigger requirements, (c) all particles passing E counter and shower shape requirements, (d) all hadrons passing the trigger requirements, and (e) all hadrons passing the cuts of (c).

combination of these cuts together with the requirement that the particle deposits all its energy in the lead–glass gives an event by event rejection of better than 1 in 10^4 (i.e., less than 1 hadron in 10^4 appears between 0.95 and 1.05 on the E/p plot and passes all the electron cuts).

Hadron rejection can be improved further in our application by doing a background subtraction. Placing two inches of lead in the secondary beam creates an effectively pure hadron beam, and figs. 8d and 8e present the E/p distributions, before and after electron cuts, for this hadron beam. This shows that there is no artificial "electron" peak produced by the cuts and the shape of the cut E/p distributions agrees very well away from the electron peak. The shape agreement outside $E/p=1$ and estimates of effects near $E/p=1$ indicate that the background under the electron peak is well measured by the 2″ Pb data. Subtraction of this background leaves us with a hadron rejection of better than 1 part in 10^5.

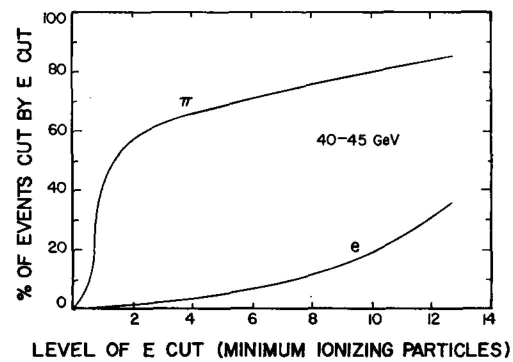

Fig. 9. Effect of E counter cut vs. number of minimum ionizing particles required for electrons and pions which leave all their energy in the lead glass.

The 2.3 radiation lengths of lead in front of the lead–glass plays an important role in the hadron rejection obtainable with the lead–glass. Hadron rejection is ultimately limited by such processes as charge exchange ($\pi^{\pm}+N\rightarrow n\pi^0+N$) where most of the energy of the charged pion goes to one or more π^0's. The π^0's immediately decay into gamma rays starting a cascade shower which is indistinguishable from an electron-initiated shower. Thus charge exchanges occurring near the front of the array cannot be separated from electrons. It is important to provide a bias against such early processes by providing that the first radiation lengths be of lead, which has a smaller number of interaction lengths per radiation length than does the lead glass, and that the shower be examined after a small number of radiation lengths.

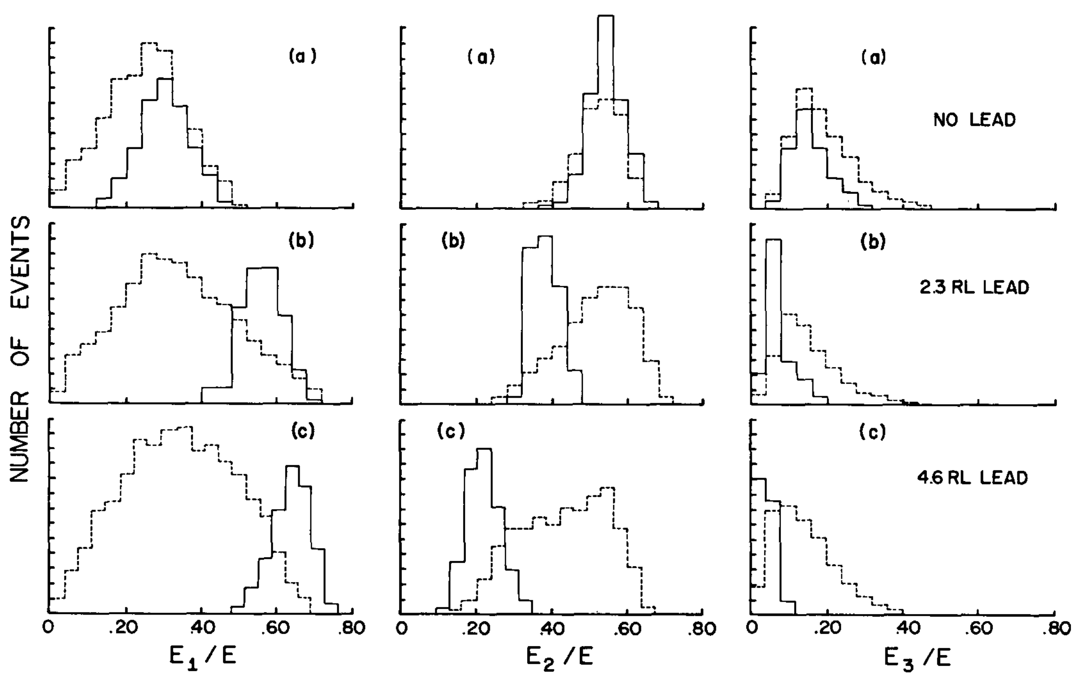

Fig. 10. Fraction of energy deposited in each layer of lead glass for the three layers (a) with no lead in front, (b) with 2.3 radiation lengths of lead as used in the experiment and (c) with 4.6 radiation lengths of lead. The solid lines are for electrons. The dashed lines are for those hadrons which deposit all their energy in the lead glass.

In our array, the lead also serves the functions of allowing cuts to be made on the E counters and of positioning the showers in the lead–glass array in such a way as to maximize the hadron rejection obtainable with the cuts on fractional energy deposition in the three layers. Fig. 10 shows the difference in the three layer depositions with various amounts of lead in front of the array. The 2.3 radiation length has no measurable effect on the resolution. However, larger amounts of lead would begin to seriously degrade the resolution.

7. Comparison to theory

Several authors[2]) have predicted the characteristics of electromagnetic showers. Analytic and Monte Carlo techniques are used to predict the particle density as a function of the depth into the showering material. In order to obtain universal expressions, materials are characterized by measuring depths in radiation lengths and curves are parameterized by a cutoff energy (e.g., the critical energy, defined as the energy for which the collision loss per radiation length equals the electron energy).

As an indication of the particle distribution, we have measured the distribution of Cherenkov energy as a function of depth in the lead–glass. This was done by inserting known thicknesses of lead in front of the lead–glass array and measuring the energy in the next 6.2, 6.2 and 14.8 radiation lengths of lead–glass. The lead served to move the shower with respect to the three layers of lead–glass.

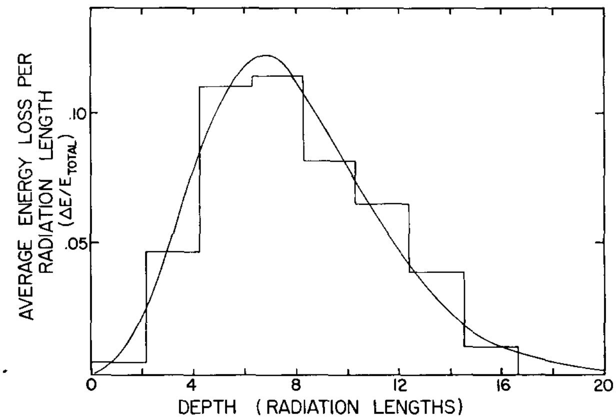

Fig. 12. Distribution of Cherenkov energy in lead–glass vs. depth for 40–45 GeV electrons. The smooth curve is obtained from analytic shower theory[3]) for the critical energy 15.8 MeV (nominal for lead–glass).

Fig. 12 shows the results of this analysis for data taken with 40–45 GeV incident electrons. For comparison, an analytic shower theory[3]) curve is given for the cutoff energy of 15.8 MeV, the nominal critical energy of the lead–glass. The curve is normalized to total area equal 1. The data shown agree better with shower theory than a similar result obtained with a lead-scintillator shower detector[4]).

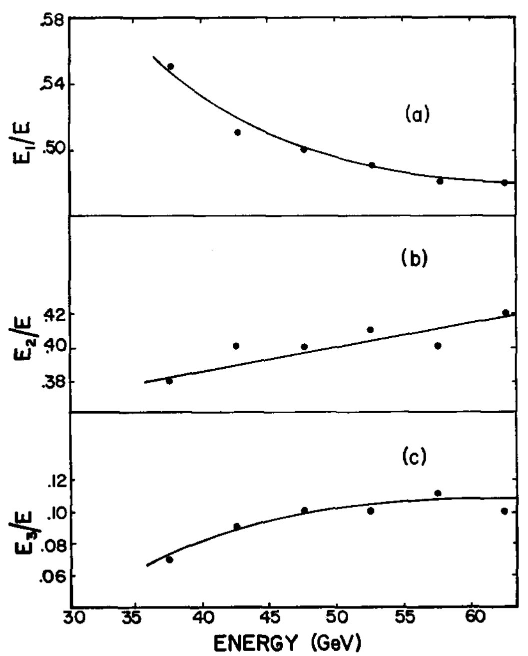

Fig. 11. Median fractional energy deposited in each layer of lead glass vs. incident energy of electronics for the first, second, and third layers (a, b and c respectively) of lead glass behind 2.3 radiation lengths of lead.

8. Recent developments

A double arm spectrometer is now being assembled at Fermilab for use in a high mass electron pair experiment. The two arrays use a total of 192 individual blocks of lead–glass; 48 blocks of the type reported on here and 144 larger SF5 blocks ($15 \times 15 \times 45\ cm^3$). These larger blocks were purchased from the same manufacturer. Their clarity and uniformity were found to be superior to the original order. Corrections for absorption along the block are significantly smaller. Curves in fig. 3 show this comparison.

We are indebted to the staff of the Wilson Electron Synchrotron and also to Professors W. Lee, N. Mistry and M. J. Tannenbaum for help in testing our original glass, to the staff of Brookhaven National Laboratory, especially D. Lazarus, for assistance in testing the assembled array and especially to the staff of the Fermi National Accelerator Laboratory for their help in setting up and testing the apparatus. We are pleased to thank the technical support of staff Nevis Laboratories and of the Fermilab Physics Department for continuing assistance. We especially acknowledge the contribution of F. W. Sippach and the Nevis Laboratories electronics group.

References

1) J. S. Beale et al., Nucl. Instr. and Meth. **117** (1974) 501; B. J. Blumenfeld et al., Nucl. Instr. and Meth. **94** (1970) 427; M. Holder et. al., Nucl. Instr. and Meth. **108** (1973) 541.

2) Analytic shower calculations: B. Rossi and K. Greisen, Rev. Mod. Phys. **13** (1941) 249; B. Rossi, *High Energy Particles* (Prentice-Hall, Englewood Cliffs, N.J., 1961); K. Kamata and J. Nishimura, Prog. Theor. Phys. **8** (1953) 93. Monte Carlo calculations: U. Völkel, DESY Report No. 65/6, 1965 (unpublished), and DESY Report No. 67/16, 1967 (unpublished).

3) Approximation A of B. Rossi, *op. cit.*

4) D. Müller, Phys. Rev. **5** (1972) 2677.